X-ray Photoelectron Spectroscopy Study of Disordering in $Gd_2(Ti_{1-x}Zr_x)_2O_7$ Pyrochlores

J. Chen, J. Lian, L. M. Wang, and R. C. Ewing*
Department of Nuclear Engineering & Radiological Sciences, University of Michigan, Ann Arbor, Michigan 48109-2104

R. G. Wang and W. Pan
State Key Laboratory of New Ceramics & Fine Processing, Department of Materials Science & Engineering, Tsinghua University, Beijing 100084, China

(Received 2 October 2001; published 20 February 2002)

The dramatic increases in ionic conductivity in $Gd_2(Ti_{1-x}Zr_x)_2O_7$ solid solution are related to disordering on the cation and anion lattices. Disordering in $Gd_2(Ti_{1-x}Zr_x)_2O_7$ was characterized using x-ray photoelectron spectroscopy (XPS). As Zr substitutes for Ti in $Gd_2Ti_2O_7$ to form $Gd_2(Ti_{1-x}Zr_x)_2O_7$ ($0.25 < x \leq 0.75$), the corresponding O 1s XPS spectrum merges into a single symmetric peak. This confirms that the cation antisite disorder occurs simultaneously with anion disorder. Furthermore, the O 1s XPS spectrum of $Gd_2Zr_2O_7$ experimentally suggests the formation of a split vacancy.

DOI: 10.1103/PhysRevLett.88.105901 PACS numbers: 66.30.Hs, 72.80.Ng, 79.60.Ht

Pyrochlore-structured oxides have become one of the most promising candidate ionic and electronic conductivity materials. Among them, the $Gd_2(Ti_{1-x}Zr_x)_2O_7$ binary is of particular interest due to its intrinisic fast oxygen ion conductivity and its potential for low temperature operation and greater compositional flexibility for materials optimization [1–3]. The easily controlled ionic conductivity has made Gd-titanate pyrochlore a candidate material for use in fuel cells, oxygen sensors, and ion pumps [4]. Furthermore, recent work has shown that pyrochlore becomes increasingly radiation resistant with increasing Zr content in $Gd_2(Ti_{1-x}Zr_x)_2O_7$ when subjected to 1 MeV Kr^+ irradiation [5–7]. This suggests the potential of expanding the use of $Gd_2(Ti_{1-x}Zr_x)_2O_7$ as an oxygen sensor in high-radiation environments. Considering the excellent conductivity properties and displacive radiation resistance of $Gd_2(Ti_{1-x}Zr_x)_2O_7$, it is also a potential material for use in fuel cells in the radiation environment of space [8].

Previous work on $Gd_2(Ti_{1-x}Zr_x)_2O_7$ pyrochlores has been mainly focused on conductivity variation as a function of different doping levels [9–11]. Only a few studies have included detailed structural characterizations [12–14]. For example, Heremans *et al.* found that the formation of cation and anion disordering occurred separately by studying the progressive changes in the structure in $Y_2(Ti_{1-x}Zr_x)_2O_7$ using neutron diffraction [14]; however, because of the strong absorption of neutrons by Gd, neutron diffraction cannot be applied to the $Gd_2(Ti_{1-x}Zr_x)_2O_7$ system. Recently, several calculations based on energy minimization with a Born-like description of the lattice have indicated that cation disordering occurs more easily than the anion disordering in the $Gd_2(Ti_{1-x}Zr_x)_2O_7$ system [15,16], but direct experimental confirmation has been lacking. Because of its sensitivity to chemical surroundings, x-ray photoelectron spectroscopy (XPS) is especially useful for the characterization of the evolution of the chemical environment of an element, especially in the case of disordered materials. We have followed the change in binding energy for oxygen in $Gd_2(Ti_{1-x}Zr_x)_2O_7$ and have analyzed the variation of O 1s electron XPS spectra as a function of changes in the Ti/Zr ratio.

The preparation of samples in the pyrochlore solid-solution series $Gd_2(Ti_{1-x}Zr_x)_2O_7$ has been described in detail elsewhere [6]. The transmission electron microscopy (TEM) observation of the samples was conducted using a JEOL 4000 EX electron microscope operated at an accelerating voltage of 400 keV. XPS investigations were performed using an ESCA LAB5 XPS spectrometer with a Mg K_α x-ray source ($h\nu = 1253.6$ eV). The samples were kept overnight in the preparation chamber, and then broken and immediately inserted into the analysis chamber of the XPS spectrometer where the vacuum was maintained at $\sim 3.7 \times 10^{-9}$ Torr. Ar^+ sputtering was used to remove carbon and other contamination from the fracture surface. The C 1s photoelectron line ($E_b = 284.6$ eV) was used to calibrate the binding energies of the photoelectron.

Figure 1(a) is the O 1s XPS spectrum of $Gd_2Ti_2O_7$. There are two peaks in the O 1s electron XPS spectrum, and the spectrum can be fitted by two Gaussian functions. The difference in binding energy of oxygen is the consequence of the difference of the effective negative charge on oxygen. The lower the binding energy, the higher the average electron density on the element. In $Gd_2Ti_2O_7$ pyrochlore, there are two different oxygen sites at 48f and 8a (with origin at Gd). Among them, six out of every seven oxygen ions occupy the 48f sites and each is coordinated by two gadolinium and two titanium ions. The other oxygen ion occupies the 8a site and is surrounded by four gadolinium ions. Considering the lower electronegativity of Gd^{3+}, as compared with that of Ti^{4+}, the ionic character of the Gd-O bond is greater than that of the Ti-O bond. This means that the electron density on oxygen for the Gd-O bond is higher than that of the Ti-O bond. Thus, we assign the peak in the O 1s spectrum with the lower binding energy to oxygen ions at 8a

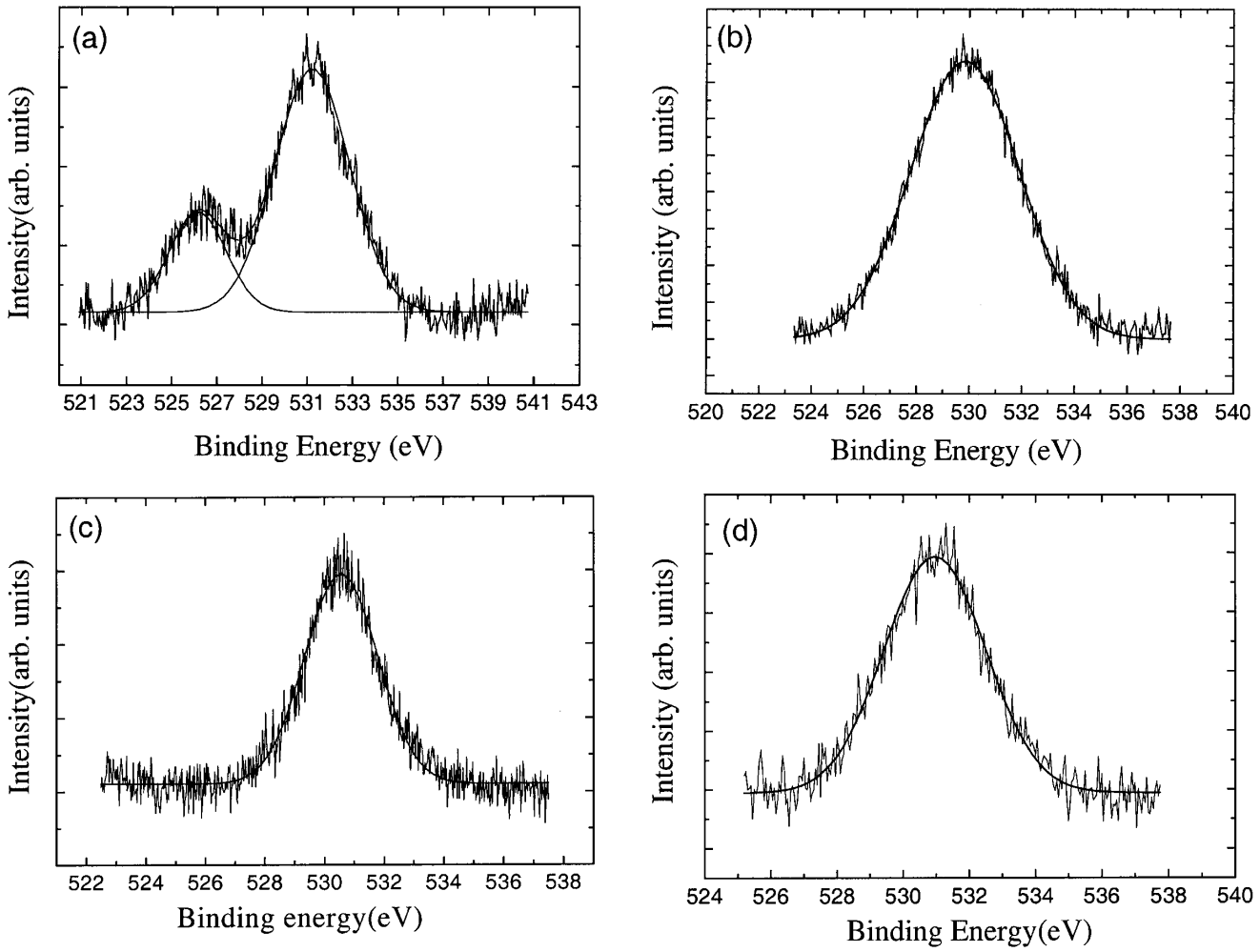

FIG. 1. O 1s XPS spectra and the corresponding Gaussian functional fitted curves of $Gd_2(Ti_{1-x}Zr_x)_2O_7$ pyrochlores: (a) $x = 0$, (b) $x = 0.25$, (c) $x = 0.5$, (d) $x = 0.75$.

sites, and the peak of the O 1s spectrum with the higher binding energy is assigned to oxygen at 48f sites. However, when 25 mol% Ti in $Gd_2Ti_2O_7$ is replaced by Zr to form $Gd_2(Ti_{0.75}Zr_{0.25})_2O_7$, the XPS spectrum of O 1s merges into one peak [Fig. 1(b)]. The peak can be fitted as a single Gaussian function. This means that the chemical environment of oxygen ions at the 48f and 8a sites has become nearly identical. The further addition of Zr does not change the symmetry of O 1s spectrum, as shown in Figs. 1(c) and 1(d), respectively.

Cation antisite and anion disorder (Frenkel pairs) are the two main disordering mechanisms in pyrochlore $A_2B_2O_7$:

$$A_A + B_B \rightarrow A'_B + B^{\cdot}_A , \quad (1)$$

$$O_O \rightarrow V^{\cdot\cdot}_{O(48f)} + O''_{i(8b)} , \quad (2)$$

where A'_B indicates the substitution of an A^{3+} cation onto a B site; $B^{\cdot}_A$ for the substitution of a B^{4+} cation onto an A site. $V^{\cdot\cdot}_{O(48f)}$ is a vacancy on a 48f site, and $O''_{i(8b)}$ is an interstitial on an 8b site in Eq. (2). For the two types of disorder, only cation disorder increases the similarity between nonequivalent oxygen sites. Thus, the similarity between these oxygen sites as revealed by this XPS study is a result of disorder on the cation antisites. This interference is consistent with the atomic simulation calculation based on energy minimization by Minervini *et al.* [15]. In their calculations, they found that the cation antisite has the lowest energy intrinsic disorder mechanism. However, the x-ray diffraction results show that $Gd_2(Ti_{1-x}Zr_x)_2O_7$ ($0 < x \leq 0.75$) is entirely in pyrochlore stability field [17]. The selected area diffraction (SAD) by TEM also shows a superlattice pattern that is evidence for the pyrochlore structure. On the other hand, close examination of the structure of $Gd_2Ti_2O_7$ shows that when there is a partial filling of cation antisites, such as the two pairs of adjacent Gd-Ti cations around 48f, the 48f, 8b, and 8a sites become crystallographically equivalent [16]. This leads to the spectrum with a single peak in the O 1s electron XPS spectrum. Because it is only partial cation disordering, the peak characteristic of the pyrochlore structure can still be found in the corresponding XRD patterns and SAD patterns by TEM. Wilde and Catlow have found that just such a switch of two pairs of adjacent cations can readily result in the Frenkel defect formation energy being reduced from

5.32 to 1.89 eV for $Gd_2Ti_2O_7$, and from 4.21 to 1.51 eV for $Gd_2Zr_2O_7$, respectively [16]. This proves that such a switch is energetically favorable.

In a study of the ionic conductivity of $Gd_2(Ti_{1-x}Zr_x)_2O_7$, Moon *et al.* have found that, at 600 °C, when $x < 0.25$, the ionic conductivity of $Gd_2(Ti_{1-x}Zr_x)_2O_7$ is nearly the same as that of $Gd_2Ti_2O_7$ [1]. When x increases from 0.25 to 0.40, the ionic conductivity increases rapidly. In addition, the activation energy is only slightly dependent on x in $Gd_2(Ti_{1-x}Zr_x)_2O_7$. This means that the ionic conductivity is primarily dependent on the preexponential constant [1]:

$$\sigma_O = \{4\alpha e^2 a_O^2 \nu_O N_O [V_O^{\cdot\cdot}] \exp(S_M/k)\}/k\,, \qquad (3)$$

where σ_O is the preexponential constant for ionic conductivity, α is a geometrical factor, e is the elementary charge, a_O is the carrier jump distance, ν_O is the jump frequency, N_O is the number of oxygen ions at the $48f$ sites per unit volume, $V_O^{\cdot\cdot}$ is the fractional oxygen $48f$ site vacancy concentration, S_M is the migration entropy, and k is Boltzmann's constant. Obviously, the preexponential constant reflects the carrier concentration. Thus, the degree of ionic conductivity in pyrochlore depends on the presence of anion disorder.

Considering the XPS results, with the effect of cation disorder in increasing anion disorder as discussed above, and the change of ion conductivity of $Gd_2(Ti_{1-x}Zr_x)_2O_7$ with x at 600 °C, it is reasonable to conclude that the onset of cation disorder begins when x equals 0.25, and anion disorder occurs simultaneously. In the study of structure evolution with Zr content in similar $Y_2(Ti_{1-x}Zr_x)_2O_7$ pyrochlore, Heremans *et al.* have found by a neutron diffraction study that the cation distribution remained remarkably ordered through the first half of the solid solution series, i.e., Y remained confined to the A site and Zr progressively replaced Ti on the B site. The onset of mixing between A and B sites began when $x \approx 0.5$ [14,18]. However, like $Gd_2(Ti_{1-x}Zr_x)_2O_7$, the conductivity of $Y_2(Ti_{1-x}Zr_x)_2O_7$ also increases rapidly when x is close to 0.25 [1]; this indicates that there is adequate anion disorder at this composition. According to our XPS results and the calculation mentioned above, which demonstrate that the anion disorder depends on the cation disorder, and considering the ionic conductivity results, it is concluded that the cation disorder already becomes evident when $x = 0.25$, rather than $x \approx 0.5$.

When titanium has been completely replaced by zirconium, a shoulder occurs on the peak at the low binding energy side of the XPS spectrum (Fig. 2). This appears to contradict the results of the O $1s$ XPS spectra tend for $Gd_2(Ti_{1-x}Zr_x)_2O_7$ ($0 \le x \le 0.75$), because the peak for $Gd_2Zr_2O_7$ should have been more symmetric than the peak for $Gd_2(Ti_{1-x}Zr_x)_2O_7$ ($0 \le x < 1$). Obviously, the unsymmetric O $1s$ XPS spectrum in $Gd_2Zr_2O_7$ cannot be the result of cation reordering because cation disordering increases with x in $Gd_2(Ti_{1-x}Zr_x)_2O_7$ ($0 \le x \le 1$) [1]. A possible explanation is the nonsymmetric location of the interstitial oxygen ions. In simulating the atomic defect structure and oxygen ion migration mechanism for $Gd_2Zr_2O_7$, van Dijik *et al.* used a "split vacancy" to explain the decreased activation enthalpy for oxygen ion conductivity as a function of ordering [19]. In the calculation, they found a $48f$ vacancy and $8b$ interstitial pair is the most stable among the possible Frenkel defects in pyrochlore. However, the possibility of the $8b$ interstitial near the $48f$ site relaxing into the latter would result in the annihilation of this Frenkel defect pair. Considering the $48f$ vacancy more closely, it appeared that a split vacancy structure could be formed. In their model, the split vacancy is formed by a $48f$ vacancy pair in the $\langle 110 \rangle$ direction with an interstitial oxygen ion located between the two vacancies. As compared with those at the $8b$ site, the surroundings of the interstitial oxygen are not symmetric, and the interstitial oxygen is closer to the two Gd^{3+} ions surrounding the $48f$ vacancy. Gd^{3+} ions have a lower electronegativity as compared with that of Ti^{4+}; thus, the surface electron density of the interstitial oxygen ion is larger than that of the $8b$ site. This may be the explanation for the shoulder on the lower binding energy side of the O $1s$ XPS spectrum in $Gd_2Zr_2O_7$. The most recent atomic simulation by Pirzada *et al.* has shown that the split vacancy becomes more and more stable with the transition from the pyrochlore to fluorite structure [20]. This calculation is consistent with our results that show a symmetric O $1s$ spectrum when $0.25 < x \le 0.75$ in $Gd_2(Ti_{1-x}Zr_x)_2O_7$, while a nonsymmetric peak occurs in the O $1s$ spectrum obtained for $Gd_2Zr_2O_7$. This reveals that the migration mechanism of oxygen in $Gd_2Zr_2O_7$ may be different from that of $Gd_2(Ti_{1-x}Zr_x)_2O_7$ ($0 \le x \le 0.75$). Apparently, the split vacancy provides more geometric flexibility for the migration of oxygen ions. This is expected to increase the preexponential factor as shown in Eq. (3), thus, resulting

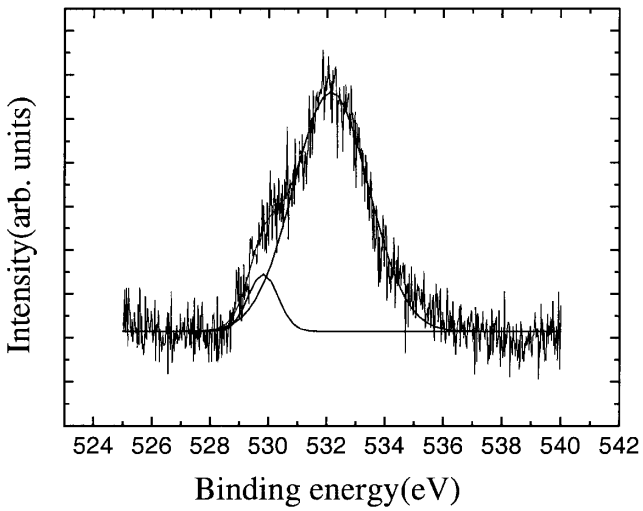

FIG. 2. O $1s$ XPS spectrum of $Gd_2Zr_2O_7$. It can be fitted by two Gaussian functional curves, indicating the different anion migration mechanism from that in $Gd_2(Ti_{1-x}Zr_x)_2O_7$.

in higher ionic conductivity. However, because the spectrum in Fig. 2 can be fitted by two Gaussian functions, it is suggested that the split vacancy makes an additional contribution to the ionic conductivity of $Gd_2Zr_2O_7$, whose conductivity mechanisms in $Gd_2(Ti_{1-x}Zr_x)_2O_7$ $(0 \leq x \leq 0.75)$ still operate in $Gd_2Zr_2O_7$.

In summary, when compared to $Gd_2Ti_2O_7$, the O $1s$ XPS spectrum of $Gd_2(Ti_{1-x}Zr_x)_2O_7$ $(0.25 \leq x \leq 0.75)$ has merged to a single symmetric peak as zirconium substitutes for titanium. Combined with the ionic conductivity results, this demonstrates that cation antisites occur simultaneously with anion disordering. The O $1s$ XPS results of $Gd_2Zr_2O_7$ suggest the existence of a split vacancy and for the first time, provide experimental support to the atomic simulation calculations that have proposed a split vacancy mechanism [19].

This work was supported by the Office of Basic Energy Sciences, U.S. DOE under DOE Grant No. DE-FG02-97ER45656 and Project No. 985 of Tsinghua University.

*Corresponding author.
Email address: rodewing@umich.edu

[1] P. K. Moon and H. L. Tuller, Mater. Res. Soc. Symp. Proc. **135**, 149 (1990).
[2] H. L. Tuller, J. Electroceram. **1**, 211 (1997).
[3] J. Lian, L. M. Wang, S. X. Wang, J. Chen, L. A. Boatner, and R. C. Ewing, Phys. Rev. Lett. **87**, 145901 (2001).
[4] H. L. Tuller, Solid State Ion. **52**, 135 (1992).
[5] S. X. Wang, L. M. Wang, R. C. Ewing, and K. V. Govindan Kutty, Mater. Res. Soc. Symp. Proc. **540**, 355 (1999).
[6] S. X. Wang, B. D. Begg, L. M. Wang, R. C. Ewing, W. J. Weber, and K. V. G. Kutty, J. Mater. Res. **14**, 4470 (1999).
[7] W. J. Weber and R. C. Ewing, Science **289**, 2501 (2000).
[8] M. Ishimar, I. V. Afanasyev-Charki, and K. E. Sickafus, Appl. Phys. Lett. **76**, 2556 (2000).
[9] P. K. Moon, M. A. Spears, and H. L. Tuller, Mater. Res. Soc. Symp. Proc. **138**, 157 (1990).
[10] P. K. Moon and H. L. Tuller, Solid State Ion. **28–30**, 470 (1988).
[11] P. K. Moon and H. L. Tuller, Sens. Actuators B **1**, 199 (1990).
[12] B. D. Begg, N. J. Hess, D. E. McCready, S. Thevuthasan, and W. J. Weber, J. Nucl. Mater. **289**, 188 (2001).
[13] M. Oueslati, M. Balkanski, P. K. Moon, and H. L. Tuller, Mater. Res. Soc. Symp. Proc. **135**, 199 (1989).
[14] C. Heremans, B. J. Wuensch, J. K. Slatick, and E. Prince, Mater. Res. Soc. Symp. Proc. **293**, 349 (1990).
[15] L. Minervini, R. W. Grimes, and K. E. Sickafus, J. Am. Ceram. Soc. **83**, 1873 (2000).
[16] P. J. Wilde and C. R. A. Catlow, Solid State Ion. **112**, 173 (1998).
[17] K. B. Helean (private communication).
[18] C. Heremans, B. J. Wuensch, J. K. Slatick, and E. Prince, J. Solid State Chem. **117**, 108 (1995).
[19] M. P. van Dijik, A. J. Burggraaf, A. N. Cormack, and C. R. A. Catlow, Solid State Ion. **17**, 159 (1985).
[20] M. Pirzada, R. W. Grimes, L. Minervini, J. F. Maguire, and K. E. Sickafus, Solid State Ion. **140**, 201 (2001).